Localization of the Activation Gate of a Voltage-gated Ca^{2+} Channel

Cheng Xie, Xiao-guang Zhen, and Jian Yang

Department of Biological Sciences, Columbia University, New York, NY 10027

Ion channels open and close in response to changes in transmembrane voltage or ligand concentration. Recent studies show that K^{+} channels possess two gates, one at the intracellular end of the pore and the other at the selectivity filter. In this study we determined the location of the activation gate in a voltage-gated Ca^{2+} channel (VGCC) by examining the open/closed state dependence of the rate of modification by intracellular methanethiosulfonate ethyltrimethylammonium (MTSET) of pore-lining cysteines engineered in the S6 segments of the α1 subunit of P/Q type Ca^{2+} channels. We found that positions above the putative membrane/cytoplasm interface, including two positions below the corresponding S6 bundle crossing in K^{+} channels, showed pronounced state-dependent accessibility to internal MTSET, reacting ∼1,000-fold faster with MTSET in the open state than in the closed state. In contrast, a position at or below the putative membrane/cytoplasm interface was modified equally rapidly in both the open and closed states. Our results suggest that the S6 helices of the α1 subunit of VGCCs undergo conformation changes during gating and the activation gate is located at the intracellular end of the pore.

INTRODUCTION

Voltage-gated ion channels respond to changes in the transmembrane voltage by opening and closing an activation gate. Using site-specific cysteine modification (Yang and Horn, 1995; Larsson et al., 1996; Liu et al., 1997; del Camino et al., 2000; Liu and Siegelbaum, 2000; del Camino and Yellen, 2001; Flynn and Zagotta, 2001), fluorescence measurement (Mannuzzu et al., 1996; Mannuzzu and Isacoff, 2000), FRET spectroscopy (Cha et al., 1999; Glauner et al., 1999), and electron paramagnetic resonance (Perozo et al., 1999; Liu et al., 2001), investigators have begun to unravel the complex conformation changes associated with gating, including the movement of the voltage sensor and the activation gate. The crystal structures of several bacterial K^{+} channels (KcsA, MthK, K$_v$AP, and KirBac) have provided particularly useful information on the molecular mechanism of gating (Doyle et al., 1998; Jiang et al., 2002a,b, 2003a,b; Kuo et al., 2003). These structures suggest that the M2/S6 transmembrane segments of K^{+} channels undergo large conformational changes during gating; they form a narrow constriction (∼5 Å in diameter) at the intracellular end when the channel is closed but widen to ∼12 Å when the channel is open.

The location of the activation gate for several types of channels has recently been explored. Based on properties of block of voltage-gated K^{+} (K$_v$) channels by organic molecules, Armstrong first proposed that the activation gate of these channels was located at the intracellular entrance to the pore (Armstrong, 1966, 1971, 1974). More recent work by studying gating-dependent changes in the rate of chemical modification of cysteines engineered on both sides of the S6 bundle crossing have provided strong support for the intracellular location of the activation gate in K$_v$ channels (Liu et al., 1997; del Camino and Yellen, 2001). The intracellular gate also acts as the activation gate in hyperpolarization-activated cation channels (Shin et al., 2001; Rothberg et al., 2002). On the other hand, another gate, denoted as the "pore gate," located at the selectivity filter, also appears to be involved in the activation gating of K$_v$ channels (Chapman et al., 1997; Zheng and Sigworth, 1997, 1998). Furthermore, the pore gate appears to be the primary activation gate in several other types of ion channels, including cyclic nucleotide–gated (CNG) channels (Liu and Siegelbaum, 2000; Flynn and Zagotta, 2001), SK-type Ca^{2+}-dependent K^{+} channels (Bruening-Wright et al., 2002), and inward rectifier K^{+} channels (Xiao et al., 2003; but see Phillips et al., 2003).

Voltage-gated Ca^{2+} channels (VGCCs) are evolutionarily related to K$_v$ channels (Hille, 2001). Although the pore of VGCCs is formed by four homologous repeats of a single α1 subunit rather than by four α subunits as in K$_v$ channels, the general features of the S4 voltage sensor and the S6 transmembrane segment are conserved. It is thus expected that VGCCs share similar gating mechanisms as K$_v$ channels. A recent study using Y^{3+} block as a tool suggests that the activation gate of the α1G T-type Ca^{2+} channel is located on the intracellular side of the selectivity filter (Obejero-Paz et al., 2004). However, the exact location of this gate and the

Abbreviations used in this paper: CNG, cyclic nucleotide–gated; MTSET, methanethiosulfonate ethyltrimethylammonium; VGCC, voltage-gated Ca^{2+} channel.

molecular movement associated with activation gating has not been determined.

In this work, we examined the location of the activation gate of the P/Q-type (Ca$_v$2.1) Ca^{2+} channel by studying the open/closed state dependence of modification by intracellular methanethiosulfonate ethyltrimethylammonium (MTSET) of engineered pore-lining cysteines in the S6 segments of the α_1 subunit. These segments form the inner pore (Zhen et al., 2005). We found that in each repeat, cysteines placed above the putative membrane/cytoplasm interface were modified ~1,000-fold faster by MTSET in the open state than in the closed state. Interestingly, two of these cysteines are located below the corresponding S6 bundle crossing in K$^+$ channels. On the other hand, a cysteine placed at the putative membrane/cytoplasm interface was modified equally rapidly in both the open and closed states. These results suggest that the S6 helices of VGCCs undergo conformation changes upon voltage changes and the activation gate is located at or below the membrane/cytoplasm interface.

MATERIALS AND METHODS

Molecular Biology and Expression of Channels in *Xenopus* Oocytes

Construction of the control channel and cysteine mutant channels was as described in the accompanying paper (Zhen et al., 2005). cRNA for all constructs (control α_1, mutant α_1, $\alpha_2\delta$, and β_{2a} subunits) were transcribed in vitro using T7 polymerase after linearization. Oocytes preparation and cRNA injection were also as described (Zhen et al., 2005).

Electrophysiology

All patch-clamp recordings were performed using the inside-out configuration. Procedures and protocols for most of the recordings were as described (Zhen et al., 2005). In some experiments where rapid solution exchange was required, solutions were delivered to the intracellular side of the membrane through a pressurized fast perfusion system (SF-77B, Warner Instruments), which under our experimental conditions, could achieve a complete exchange of solution in ~150 ms.

Macroscopic currents were evoked from a holding potential of −80 mV every 6 s by a 500-ms depolarization to +20 or +30 mV. In experiments to determine the voltage dependence of modification of K$^+$ currents, the holding potential was set at −100 mV and currents were evoked by depolarization to different voltages, from −80 to +40 mV. For closed-state modification using regular perfusion, current was evoked by a 20-ms depolarization to +20 or +30 mV before and after application of MTSET, which was applied for 1–2 min and subsequently washed out for 1 min. When pressurized fast perfusion was used, current was evoked every 20 s by a 20-ms depolarization to +20 mV. MTSET was applied for 10 s in between the test pulses. For closed-state modification of IIS6-D0C, current was evoked every 10 s by a 20-ms depolarization to +10 mV and MTSET was applied for 4 s in between the test pulses. Currents were filtered at 2 kHz, digitized at 10 kHz. Data acquisition and analysis were performed using pClamp8 (Axon Instruments) on a PC through a Digidata 1200 interface. Experiments were performed at 21–23°C.

```
                                  25                 1 0  −3
                                  |                  | | |
Ca_v2.1  IS6    336   NWLYFIPLIIIGSFFMLNLVLGVLSGEFA 364
         IIS6   690   FSIYFIVLTLFGNYTLLNVFLAIAVDNLA 718
         IIIS6  1496  MSIFYVVYFVVFPFFFVNIFVALIIITFQ 1524
         IVS6   1796  AYFYFVSFIFLCSFLMLNLFVAIMDNFE 1824

                                                 ↓
KcsA     M2     88    GRLVAVVVMVAGITSFGLVTAALATWFVG 116
Shaker   S6     455   GKIVGSLCVVAGVLTIALPVPVIVSNFNY 483
```

Figure 1. Pore-lining residues in S6. Amino acid sequence alignment of the four S6 segments in the Ca$_v$2.1 subunit and the M2/S6 segment of KcsA and *Shaker* K$^+$ channels. Amino acid numbers are given on both sides. For Ca^{2+} channel S6 segments, the amino acid numbering defined in this study is shown on the top. Position 0 presumably represents the membrane/cytoplasm interface. Bold positions denote those that can be modified by internal MTSET. Underlined positions were studied in this work. For K$^+$ channel M2/S6 segments, bold residues denote pore-lining positions defined either structurally or by MTS reagent accessibility. Arrow marks the M2/S6 bundle crossing.

No corrections were made for leakage current, which was negligible in macropatch recordings, or for channel rundown, which was greatly reduced by inclusion of 2 mM Mg-ATP and 3 µM PIP$_2$ in the intracellular solution. The time constant of modification was obtained by fitting the time course of modification with a single exponential function. The apparent second-order rate constant of MTSET reaction with a cysteine mutant channel was then calculated as the reciprocal of the time constant divided by the MTSET concentration. To determine the appropriate concentration of MTSET to use, we examined the relationship between MTSET concentration and its modification rate on the IIS6-A4C channel. At the voltage that opens 80% of the channels, the relationship was linear between 0.5 and 2 mM but reached a plateau at 3 mM (not depicted). Therefore, 1 mM MTSET was used for most of the open- and closed-state modification experiments. In experiments to determine the voltage dependence of MTSET modification (Fig. 5), different concentrations (0.5, 1, or 2 mM) of MTSET were used at different voltages in order to obtain a more accurate estimate of the second-order rate constants. MTSET (Toronto Research Chemicals) was stored at −20°C and was dissolved in the control solution before each experiment, generally <5 min before application.

To determine the closed-state modification rate for IIS6-D0C, we used the fast perfusion system mentioned above to apply MTSET only in the closed state. The time course of modification was plotted against the cumulative MTSET exposure time in the closed state, which was then fitted with a single exponential to get the time constant and the closed-state rate. The open-state modification rate was calculated by subtracting the closed-state rate from the rate obtained in both the open and closed states.

RESULTS

State-dependent Modification of Pore-lining Cysteines Engineered in S6

Using the substituted cysteine accessibility method, we have identified many pore-lining positions in the S6 transmembrane segment in each repeat (Zhen et al., 2005). These positions are highlighted in the amino acid sequence alignment of the four S6 segments of Ca$_v$2.1 (Fig. 1), where position 0 is presumed to lie at
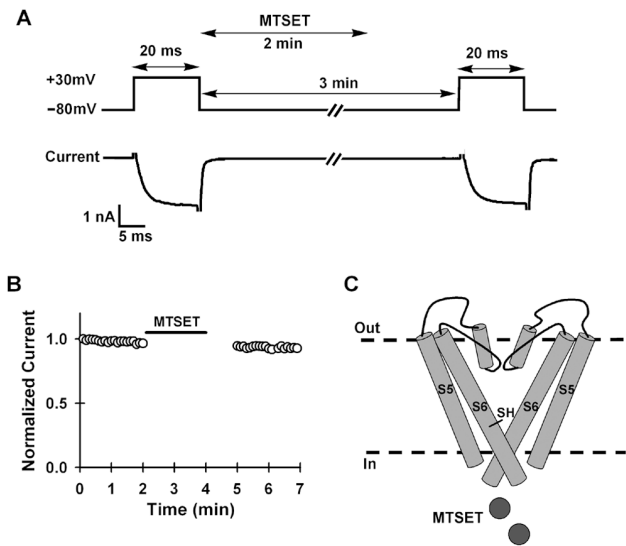
Figure 2. Closed-state modification of a cysteine above the putative membrane/cytoplasm interface. (A) Voltage protocol for closed-state modification by internal MTSET and representative current traces. Current was evoked by a 20-ms test pulse before and after MTSET (1 mM) application. Voltage was held at −80 mV when MTSET was applied for 2 min and then washed out for 1 min. (B) An exemplar time course of closed-state modification of IIIS6-V9C. Each point represents the peak current evoked by the 20-ms test pulse. Pulsing was stopped during MTSET application and washout. (C) Cartoon of S5 and S6 transmembrane helices and P-loop in the closed state. The thiol group of a pore-lining cysteine above the membrane/cytoplasm interface is shown. Dark gray spheres represent MTSET molecules.

Figure 3. Open-state modification of a cysteine above the putative membrane/cytoplasm interface. (A) Voltage protocol for open-state modification by internal MTSET and representative current traces. Current was evoked every 6 s by a 500-ms test pulse. MTSET (1 mM) was applied continuously in both the open and closed states until steady-state inhibition was reached. (B) An exemplar time course of open-state modification of IIIS6-V9C. (C) Cartoon of S5 and S6 transmembrane helices and P-loop in the open state. The thiol group of a pore-lining cysteine above the membrane/cytoplasm interface is shown. Dark gray spheres represent MTSET molecules.

the membrane/cytoplasm interface and residues in the membrane are defined as 1, 2, 3, etc., from the intracellular side to the extracellular side. Fig. 1 also aligns the Ca$_v$2.1 S6 segments with the M2/S6 segment of two different types of K$^+$ channels (adopted from Lipkind and Fozzard, 2003). According to this alignment, the S6 bundle crossing of the K$^+$ channels is located three amino acids above the membrane/cytoplasm interface.

Based on our previous work (Zhen et al., 2005), we selected several cysteine mutant channels (including IS6-L5C, IIS6-V1C, IIS6-A2C, IIS6-A4C, and IIIS6-V9C) that were rapidly and almost completely modified by internal MTSET when it was applied continuously in both the open and closed states. We first examined modification by internal MTSET of IIIS6-V9C in the closed state (Fig. 2). Channel activity was recorded in inside-out membrane patches and was monitored by a brief (2 ms) depolarization to +30 mV from a holding potential of −80 mV. MTSET (1 mM) was applied for 2 min to the intracellular side only when channels were closed. The decrease in current, if any, was considered to be caused solely by MTSET modification in the closed state. There was only a slight decrease in current amplitude after MTSET application (Fig. 2 B), indicating that there was little modification of IIIS6-V9C in the

closed state. By contrast, IIIS6-V9C was modified irreversibly and rapidly when MTSET was applied continuously in both the open and closed states (Fig. 3). Together, these results indicate that IIIS6-V9C can be modified only when the channel is open. The open-state modification could also be seen during the depolarizing test pulse, as reflected by the faster current decay (Fig. 3 A).

Cysteines engineered in other repeats, such as IS6-L5C and IIS6-A4C, also showed no observable or only slight modification in the closed state but significant and rapid modification in the open state. These two positions are more intracellular, but they are still located above the putative membrane/cytoplasm interface.

To calculate the modification rate in the closed state, we assume that current decay during MTSET application follows a single exponential. Using the current amplitude obtained before and after MTSET application, we calculated the time constant of the current decay and then the second-order rate constant, which was less or ∼1 M^{-1}s^{-1} for all the positions situated above the putative membrane/cytoplasm interface.

We also examined closed-state modification of IIS6-A4C and IIIS6-V9C by applying MTSET in the closed state between brief test pulses (see voltage and MTSET application protocol in Fig. 4 A) through a pressurized fast perfusion system. The time course of modification was very slow (Fig. 4 B). By fitting the current decay
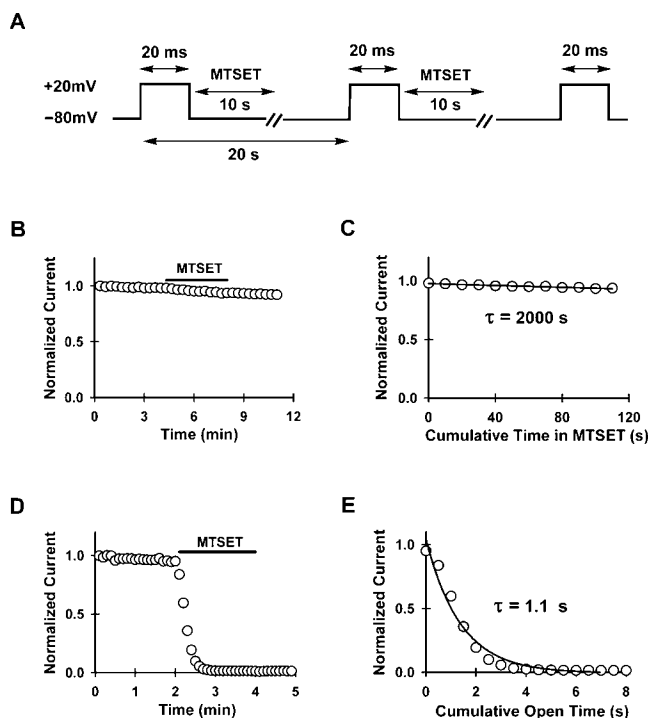
Figure 4. Comparison of open- and closed-state modification of a cysteine above the putative membrane/cytoplasm interface. (A) Voltage protocol for closed-state modification using fast perfusion. Current was evoked every 20 s by a 20-ms test pulse. Between the test pulses MTSET (1 mM) was applied for 10 s and subsequently washed out for 10 s. (B and D) Time course of MTSET modification of a representative cysteine (IIS6-A4C) in closed state (B) and open state (D). (C and E) The MTSET inhibition phase in B and D plotted against the cumulative time in MTSET or the cumulative channel open time, respectively, superimposed with a single-exponential fitting curve.

phase during MTSET application with a single exponential (Fig. 4 C), we obtained a second-order rate constant of 0.5 $M^{-1}s^{-1}$, the same as that obtained with the method described above.

Since modification of positions above the putative membrane/cytoplasm interface in the closed state was very slow and could be neglected, the time course of modification in the open state could be approximated by plotting the peak current evoked by each depolarizing pulse against the cumulative channel open time

(Fig. 4, D and E). The current decay could be well fitted by a single exponential function (Fig. 4 E), from which the second-order rate constant of MTSET modification in the open state was calculated. Fig. 5 A summarizes the apparent second-order rate constants of MTSET modification in both the open and closed states for selected mutant channels. For most positions located above the putative membrane/cytoplasm interface, the rate constants in the open state were ~1,000-fold faster than those in the closed state, suggesting that there is a physical barrier for MTSET diffusion at or below the putative membrane/cytoplasm interface.

To confirm that this marked state dependence of modification rate was related to channel gating rather than to the intrinsic voltage dependence of movement of MTSET into the inner pore, we examined the voltage dependence of MTSET modification of K^+ currents mediated by a representative mutant channel, IIS6-A4C. The reason for using K^+ current for this experiment is that compared with Ba^{2+} current the voltage dependence of activation is negatively shifted, so that we could avoid using extreme positive voltages that are harmful to the membrane. Fig. 6 shows the second-order rate constants obtained at different voltages, together with the activation curve. It is clear that the change in modification rate correlates reasonably well with channel open probability. At −80 mV, when 99% of the channels were closed, modification was very slow. At −20 mV, when 85% of the channels were open, modification was ~120-fold faster than at −80 mV. This large increase in the modification rate is apparently a consequence of channel gating. On the other hand, the modification rate increased by only ~1.3-fold between −20 and +40 mV, when channel open probability reached maximum. This small increase indicates that MTSET diffusion into the inner pore has little intrinsic voltage dependence.

The Gate for MTSET Is At or Below the Membrane/Cytoplasm Interface

The strong state-dependent modification of positions above the putative membrane/cytoplasm interface (Fig. 5 A) suggests that there is a gate for MTSET below
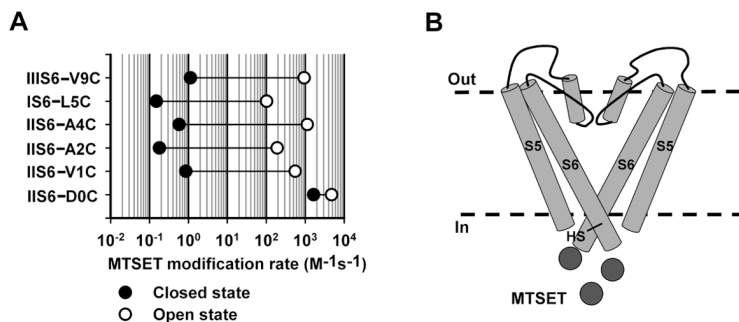
Figure 5. MTSET modification rates in open and closed states. (A) Apparent second-order rate constants for MTSET modification of selected pore-lining residues. Filled circles represent rate constants measured in the closed state (−80 mV) and open circles represent those measured in the open state (at +20 or +30 mV for different mutant channels). (B) Cartoon of the closed-state conformation of S5 and S6 helices, showing that cysteines below the membrane/cytoplasm interface can be accessed by MTSET (dark gray spheres) in the closed state.
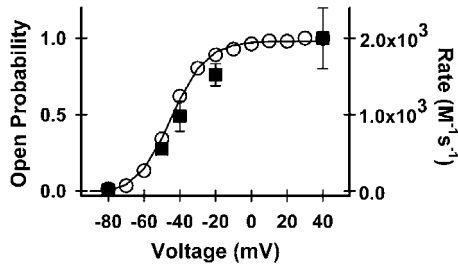
Figure 6. Voltage dependence of MTSET modification. Data were collected from IIS6-A4C. Filled squares and open circles represent, respectively, the mean modification rates ($n = 3$–5) and channel open probability measured at different voltages. The solid line is the Boltzmann fit to the voltage-activation curves obtained from 10 experiments (midpoint $= -44.8 \pm 0.6$ mV and slope factor $= 9.6 \pm 0.5$ mV).

these positions. Where exactly is this gate? To address this question, we examined MTSET modification of three continuous positions in IIS6, at or above the putative membrane/cytoplasm interface. The apparent second-order rate constants for these positions in both the open and closed states are shown in Fig. 5 A. IIS6-A2C and IIS6-V1C both showed strong state-dependent modification, with the rate being ~1,000-fold faster in the open state than in the closed state. In contrast, IIS6-D0C was modified rapidly in both the open and closed states, with only a threefold difference between the modification rates. More important, the closed-state modification rate of IIS6-V1C and IIS6-A2C is >1,000-fold slower than that of IIS6-D0C, suggesting that the gate for MTSET diffusion is situated between position 0 and 1 of IIS6, right at the putative membrane/cytoplasm interface.

Trapping of MTSET Also Suggests an Intracellular Gate

In many channels, blocking molecules are often trapped in the pore when the channel is closed (e.g., Armstrong, 1966, 1971, 1974; Holmgren et al., 1997; Shin et al., 2001; for review see Hille 2001), a phenomenon indicative of an intracellular gate. Does trapping occur to MTSET in VGCCs? To address this question, we compared MTSET modification of IIS6-A4C using two different voltage protocols, in which the magnitude of the test pulse (+30 mV) and the pulse interval (6 s) were maintained the same but the duration of the test pulse was set at 500 ms in one case and 10 ms in another (Fig. 7 A). IIS6-A4C was chosen because it exhibited little modification in the closed state (Fig. 5 A). This mutant channel was modified with both voltage protocols, but the modification was much faster with the 500-ms test pulse than with the 10-ms test pulse for the same number of test pulses (Fig. 7 B). This is expected if modification occurs predominantly in the open state. However, when the time course of modification was plotted using the cumulative channel open time, it became ap-
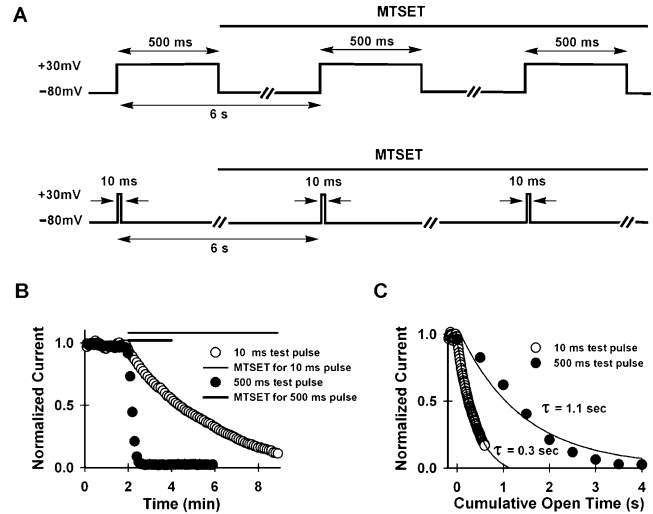
Figure 7. Trapping of MTSET in the inner pore in the closed state. (A) Two voltage protocols for measuring MTSET modification. Currents were evoked by a depolarizing pulse to +30 mV every 6 s from a holding potential of −80 mV. The duration of the depolarizing pulse was either 500 ms or 10 ms. (B) Time course of MTSET inhibition of currents evoked by the 500-ms test pulse (filled circles) or the 10-ms test pulse (open circles) in the IIS6-A4C mutant channel. (C) The MTSET inhibition phase in B plotted against the cumulative channel open time, superimposed with a single-exponential fitting curve with the indicated time constant.

parent that the modification was significantly faster (approximately fourfold) with the 10-ms test pulse (Fig. 7 C). One potential factor contributing to this apparent faster modification is the time (2–3 ms) taken for the open channels to completely close, which would increase the actual cumulative channel open time for the 10-ms test pulse by 20–30% (2–3 ms adds little to the 500-ms test pulse). However, this addition would increase the modification rate by only 20–30%. Furthermore, since 2–3 ms was also needed for all the channels to open, the real open time for the 10-ms test pulse should remain more or less 10 ms. A more likely explanation is trapping: MTSET enters the inner pore when the channel is open; it then gets trapped in the inner pore when an intracellular gate is closed and reacts with the cysteine while the channel remains in the closed state. Since more trapping events occur with the 10-ms test pulse for the same cumulative channel open time, the apparent modification rate becomes faster. Trapping in another way supports the existence of an intracellular gate.

DISCUSSION

The rationale for using the open/closed state dependence of modification of engineered pore-lining cysteines by a sulfhydryl-specific reagent to locate the channel activation gate is straightforward (del Camino and Yellen, 2001; Flynn and Zagotta, 2001): cysteines

situated above the gate would be modified much more rapidly by an internally applied modifying reagent in the open state than in the closed state, but cysteines situated below the gate would be modified equally rapidly in both the open and closed states. If there is no intracellular gate, all the cysteines along the inner pore would be modified similarly in both the open and closed states. A critical assumption for using this method to locate the activation gate is that the intrinsic reactivity of the engineered cysteine does not change with gating. This assumption is difficult to test directly, but the strong state-dependent modification of cysteines above the putative membrane/cytoplasm interface in three different S6 segments and the clear-cut difference between those cysteines and IIS6-D0C (Fig. 5 A) suggest that such an assumption is a reasonable one.

The second-order rate constant for MTSET modification in the open state is two to three orders of magnitude lower than that for MTSET modification of free thiols (Stauffer and Karlin, 1994) and of cysteines in S6 of the *Shaker* K^+ channel (Liu et al., 1997; del Camino and Yellen, 2001). Multiple reasons could account for this low rate, including the low intrinsic reactivity of the engineered cysteines and the low open probability of P/Q-type Ca^{2+} channels. Similar low rates have also been reported for cysteines in M2 of Kir channels (Phillips et al., 2003; Xiao et al., 2003), S6 of SK-type Ca^{2+}-dependent K^+ channels (Bruening-Wright et al., 2002), and S6 of CNG channels (Flynn and Zagotta, 2001). For the purpose of locating the activation gate, the critical measure is not the absolute rate of modification but the difference of this rate between the open and closed states. For cysteines above the membrane/cytoplasm interface, we observed an ~1,000-fold difference in the modification rate between the open and closed states. The actual difference could be significantly bigger than what we estimated. In our calculation, we assumed that the current decay in the closed state following MTSET application was totally caused by modification in closed state. However, this small decrease of current (e.g., Fig. 2 B and Fig. 4 B) could be largely due to channel rundown. Thus the closed-state modification rate we estimated is an upper limit. For positions below the putative activation gate, we suppose that MTSET access is not gated but that there is a gating-associated movement of the S6 helices, which results in a small change in the modification rate (e.g., threefold difference between the open and closed states for IIS6-D0C). This small change in cysteine reactivity with gating has been seen in the lower S6 of K_v channels (Liu et al., 1997).

The strong state-dependent modification by MTSET of cysteines above the membrane/cytoplasm interface suggests that the S6 helices form a narrow constriction at the intracellular end of pore. Where is this constriction? In KcsA, the M2 bundle crossing forms the narrowest part of the inner pore (Doyle et al., 1998). This bundle crossing also forms the activation gate in the *Shaker* K^+ channel: I477C, which lies at the bundle crossing (Fig. 1), shows strong state-dependent modification by internal MTSET but V478C, a position immediately below the bundle crossing, does not (Liu et al., 1997; del Camino and Yellen, 2001). Notably, in the P/Q-type Ca^{2+} channel, IIS6-A2C and IIS6-V1C both show strong state-dependent modification (Fig. 5 A). These two positions are located below the corresponding M2/S6 bundle crossing in K^+ channels, according to the alignment in Fig. 1. This means that either this alignment is inappropriate or the location of the activation gate in VGCCs is different from that in the *Shaker* K^+ channel. Although the details of the alignment in Fig. 1 may need revision, placing position 0 at the membrane/cytoplasm interface or even slightly below it seems appropriate, based on the hydrophobicity and the effect and pattern of MTSET modification of the amino acids below (i.e., more intracellular to) this position (see Fig. 3 of Zhen et al., 2005). Thus, we propose that the activation gate in VGCCs is located more intracellularly than that in the *Shaker* K^+ channel.

Does the constriction that gates MTSET diffusion also gate Ca^{2+} conduction? An ideal and direct experiment to answer this question is to study the open/closed state dependence of block by internal Cd^{2+}. Cd^{2+} binds to the EEEE locus in the selectivity filter with a high affinity (Yang et al., 1993), but since this effect is rapidly reversible, we cannot capitalize on this binding. However, Cd^{2+} interacts strongly with sulfhydryl groups, preferably organized in a tetrahedral geometry, and this interaction is generally extremely slow to reverse. This property has been exploited to study gating in other types of channels (Holmgren et al., 1998; del Camino and Yellen, 2001; Enkvetchakul et al., 2001; Loussouarn et al., 2001; Rothberg et al., 2002, 2003; Xiao et al., 2003; Webster et al., 2004). We also attempted to create a slowly reversible Cd^{2+} binding site in the Ca^{2+} channel pore by engineering two or four pore-lining cysteines at several analogous positions of the four S6 segments or by substituting one or two glutamates in the selectivity filter with cysteines. Unfortunately, our attempts were not successful due to several difficulties. First of all, because of the low membrane expression of Ca^{2+} channels in mammalian cell lines, all of our experiments were performed in *Xenopus* oocytes, which contain high levels of Ca^{2+}-activated Cl^- channels on the surface membrane. To avoid contamination from these channels, which can be activated by Ba^{2+} as well, albeit to a lesser degree, we used K^+ as the charge carrier. But the contaminating Ca^{2+} in the intracellular solution (presumably mainly from our

deionized water) was sufficient to activate the endogenous Ca^{2+}-activated Cl^- channels. Use of a Ca^{2+} chelator would not alleviate this problem since common chelators such as EGTA, EDTA, and BAPTA bind Cd^{2+} much more tightly than Ca^{2+}, leaving any contaminating Ca^{2+} unbuffered. We thus resorted to use a "Ca^{2+} sponge" (Yang et al., 1993) to remove the contaminating Ca^{2+} from the intracellular solution. However, even with this maneuver, we still encountered large and variable Cl^- currents because, surprisingly, Cd^{2+} itself could activate the Cl^- current. We were therefore left with a low-probability chance of encountering oocytes with no or a very low level of endogenous Ca^{2+}-activated Cl^- channels. Furthermore, all quadruple cysteine mutant channels failed to produce a large enough macroscopic current. Although some single and double mutant channels expressed well, we were still unable to carry out the Cd^{2+} block experiments due to the aforementioned technical difficulty.

Despite the lack of direct supporting data, we propose that the intracellular gate that hinders MTSET diffusion is also a gate for Ca^{2+}, because Ca^{2+} ions are most likely hydrated, at least partially, when they pass through the bundle crossing, and the size of a partially hydrated Ca^{2+} ion is similar to or larger than that of MTSET.

In the accompanying study, we concluded that the inner pore of VGCCs can open to >10 Å (Zhen et al., 2005). The closed channel is likely much narrower than this. Thus the S6 helices must undergo significant conformational changes during gating, as in K^+ channels. But do Ca^{2+} channels open the pore like K^+ channels do? A highly conserved glycine residue is present in the M2/S6 helix of various K^+ channels and closely related CNG channels. It has been proposed (Jiang et al., 2002b) that this glycine acts as a flexible gating hinge, allowing the M2/S6 inner-pore helices to form a narrow constriction as in the KcsA structure and to splay wide open as in the MthK structure. However, it has been suggested recently (Webster et al., 2004) that unlike predictions from the MthK structure, the inner-pore helices of the *Shaker* K^+ channel maintain the KcsA-like bundle-crossing motif in both open and closed states, with a bend at the Pro-X-Pro sequence, which is located above the bundle crossing and is conserved in K_v channels but not in inward rectifier K^+ channels and the bacterial K^+ channels. The implication of these studies is that the M2/S6 inner-pore helices may undergo different kinds of gating conformation changes in different types of K^+ channels. In VGCCs, a conserved glycine is present in IS6 and IIS6 but not in IIIS6 and IVS6, at a position close or analogous to the conserved glycine in K^+ channels. There is no Pro-X-Pro sequence in any of the S6 helices. It is thus expected that the gating motions of the S6 helices of VGCCs would be different from those of K^+ channels.

REFERENCES

Armstrong, C.M. 1966. Time course of TEA^+-induced anomalous rectification in squid giant axons. *J. Gen. Physiol.* 50:491–503.

Armstrong, C.M. 1971. Interaction of tetraethylammonium ion derivatives with potassium channels of giant axons. *J. Gen. Physiol.* 58:413–437.

Armstrong, C.M. 1974. Ionic pores, gates, and gating currents. *Q. Rev. Biophys.* 7:179–210.

Bruening-Wright, A., M.A. Schumacher, J.P. Adelman, and J. Maylie. 2002. Localization of the activation gate for small conductance Ca^{2+} activated K^+ channels. *J. Neurosci.* 22:6499–6506.

Cha, A., G.E. Snyder, P.R. Selvin, and F. Bezanilla. 1999. Atomic scale movement of the voltage-sensing region in a potassium channel measured via spectroscopy. *Nature.* 402:809–813.

Chapman, M.L., H.M.A. VanDongen, and A.M.J. VanDongen. 1997. Activation-dependent subconductance levels in the drk1 K channel suggest a subunit basis for ion permeation and gating. *Biophys. J.* 72:708–719.

del Camino, D., and G. Yellen. 2001. Tight steric closure at the intracellular activation gate of a voltage-gated K^+ channel. *Neuron.* 32:649–656.

del Camino, D., M. Holmgren, Y. Liu, and G. Yellen. 2000. Blocker protection in the pore of a voltage-gated K^+ channel and its structural implications. *Nature.* 403:321–325.

Doyle, D.A., J.M. Cabral, R.A. Pfuetzner, A.L. Kuo, J.M. Gulbis, S.L. Cohen, B.T. Chait, and R. MacKinnon. 1998. The structure of the potassium channel: molecular basis of K^+ conduction and selectivity. *Science.* 280:69–77.

Enkvetchakul, D., G. Loussouarn, E. Makhina, and C.G. Nichols. 2001. ATP interaction with the open state of the K-ATP channel. *Biophys. J.* 80:719–728.

Flynn, G.E., and W.N. Zagotta. 2001. Conformational changes in S6 coupled to the opening of cyclic nucleotide-gated channels. *Neuron.* 30:689–698.

Glauner, K.S., L.M. Mannuzzu, C.S. Gandhi, and E.Y. Isacoff. 1999. Spectroscopic mapping of voltage sensor movement in the Shaker potassium channel. *Nature.* 402:813–817.

Hille, B. 2001. Ion Channels of Excitable Membranes. Third edition. Sinauer Associates, Inc., Sunderland, MA. 814 pp.

Holmgren, M., P.L. Smith, and G. Yellen. 1997. Trapping of organic blockers by closing of voltage-dependent K^+ channels - evidence for a trap door mechanism of activation gating. *J. Gen. Physiol.* 109:527–535.

Holmgren, M., K.S. Shin, and G. Yellen. 1998. The activation gate of a voltage-gated K^+ channel can be trapped in the open state by an intersubunit metal bridge. *Neuron.* 21:617–621.

Jiang, Y., A. Lee, J.Y. Chen, M. Cadene, B.T. Chait, and R. MacKinnon. 2002a. Crystal structure and mechanism of a calcium-gated potassium channel. *Nature.* 417:515–522.

Jiang, Y., A. Lee, J.Y. Chen, M. Cadene, B.T. Chait, and R. MacKinnon. 2002b. The open pore conformation of potassium channels. *Nature.* 417:523–526.

Jiang, Y., A. Lee, J.Y. Chen, V. Ruta, M. Cadene, B.T. Chait, and R. MacKinnon. 2003a. X-ray structure of a voltage-dependent K^+

channel. *Nature*. 423:33–41.

Jiang, Y., V. Ruta, J.Y. Chen, A. Lee, and R. MacKinnon. 2003b. The principle of gating charge movement in a voltage-dependent K$^+$ channel. *Nature*. 423:42–48.

Kuo, A., J.M. Gulbis, J.F. Antcliff, T. Rahman, E.D. Lowe, J. Zimmer, J. Cuthbertson, F.M. Ashcroft, T. Ezaki, and D.A. Doyle. 2003. Crystal structure of the potassium channel KirBac1.1 in the closed state. *Science*. 300:1922–1926.

Larsson, H.P., O.S. Baker, D.S. Dhillon, and E.Y. Isacoff. 1996. Transmembrane movement of the Shaker K$^+$ channel S4. *Neuron*. 16:387–397.

Lipkind, G.M., and H.A. Fozzard. 2003. Molecular modeling of interactions of dihydropyridines and phenylalkylamines with the inner pore of the L-type Ca^{2+} channel. *Mol. Pharmacol*. 63:499–511.

Liu, J., and S.A. Siegelbaum. 2000. Change of pore helix conformational state upon opening of cyclic nucleotide-gated channels. *Neuron*. 28:899–909.

Liu, Y., M. Holmgren, M.E. Jurman, and G. Yellen. 1997. Gated access to the pore of a voltage-dependent K$^+$ channel. *Neuron*. 19:175–184.

Liu, Y.S., P. Sompornpisut, and E. Perozo. 2001. Structure of the KcsA channel intracellular gate in the open state. *Nat. Struct. Biol*. 8:883–887.

Loussouarn, G., L.R. Phillips, R. Masia, T. Rose, and C.G. Nichols. 2001. Flexibility of the Kir6.2 inward rectifier K$^+$ channel pore. *Proc. Natl. Acad. Sci. USA*. 98:4227–4232.

Mannuzzu, L.M., M.M. Moronne, and E.Y. Isacoff. 1996. Direct physical measure of conformational rearrangement underlying potassium channel gating. *Science*. 271:213–216.

Mannuzzu, L.M., and E.Y. Isacoff. 2000. Independence and cooperativity in rearrangements of a potassium channel voltage sensor revealed by single subunit fluorescence. *J. Gen. Physiol*. 115:257–268.

Obejero-Paz, C.A., I.P. Gray, and S.W. Jones. 2004. Y^{3+} block demonstrates an intracellular activation gate for the α1G T-type Ca^{2+} channel. *J. Gen. Physiol*. 124:631–640.

Perozo, E., D.M. Cortes, and L.G. Cuello. 1999. Structural rearrangements underlying K$^+$-channel activation gating. *Science*.

285:73–78.

Phillips, L.R., D. Enkvetchakul, and C.G. Nichols. 2003. Gating dependence of inner pore access in inward rectifier K$^+$ channels. *Neuron*. 37:953–962.

Rothberg, B.S., K.S. Shin, P.S. Phale, and G. Yellen. 2002. Voltage-controlled gating at the intracellular entrance to a hyperpolarization-activated cation channel. *J. Gen. Physiol*. 119:83–91.

Rothberg, B.S., K.S. Shin, and G. Yellen. 2003. Movements near the gate of a hyperpolarization-activated cation channel. *J. Gen. Physiol*. 122:501–510.

Shin, K.S., B.S. Rothberg, and G. Yellen. 2001. Blocker state dependence and trapping in hyperpolarization-activated cation channels: evidence for an intracellular activation gate. *J. Gen. Physiol*. 117:91–101.

Stauffer, D.A., and A. Karlin. 1994. Electrostatic potential of the acetylcholine binding sites in the nicotinic receptor probed by reactions of binding-site cysteines with charged methanethiosulfonates. *Biochemistry*. 33:6840–6849.

Webster, S.M., D. del Camino, J.P. Dekker, and G. Yellen. 2004. Intracellular gate opening in Shaker K$^+$ channels defined by high-affinity metal bridges. *Nature*. 428:864–868.

Xiao, J., X.G. Zhen, and J. Yang. 2003. Localization of PIP$_2$ activation gate in inward rectifier K$^+$ channels. *Nat. Neurosci*. 6:811–818.

Yang, J., P.T. Ellinor, W.A. Sather, J.F. Zhang, and R.W. Tsien. 1993. Molecular determinants of Ca^{2+} selectivity and ion permeation in L-type Ca^{2+} channels. *Nature*. 366:158–161.

Yang, N., and R. Horn. 1995. Evidence for voltage-dependent S4 movement in sodium-channels. *Neuron*. 15:213–218.

Zhen, X., C. Xie, A. Fitzmaurice, C.E. Schoonover, E.T. Orenstein, and J. Yang. 2005 Functional architecture of the inner pore of a voltage-gated Ca^{2+} channel. *J. Gen. Physiol*. 126:193–204.

Zheng, J., and F.J. Sigworth. 1997. Selectivity changes during activation of mutant Shaker potassium channels. *J. Gen. Physiol*. 110:101–117.

Zheng, J., and F.J. Sigworth. 1998. Intermediate conductances during deactivatian of heteromultimeric Shaker potassium channels. *J. Gen. Physiol*. 112:457–474.